Science Immunology
AAAS

Supplementary Materials for

Transmembrane domain–driven PD-1 dimers mediate T cell inhibition

Elliot A. Philips *et al.*

Corresponding author: Xiang-Peng Kong, xiangpeng.kong@nyulangone.org;
Jun Wang, jun.wang@nyulangone.org; Michael L. Dustin, michael.dustin@kennedy.ox.ac.uk

Sci. Immunol. **9**, eade6256 (2024)
DOI: 10.1126/sciimmunol.ade6256

The PDF file includes:

Figs. S1 to S10

Other Supplementary Material for this manuscript includes the following:

Data file S1
MDAR Reproducibility Report

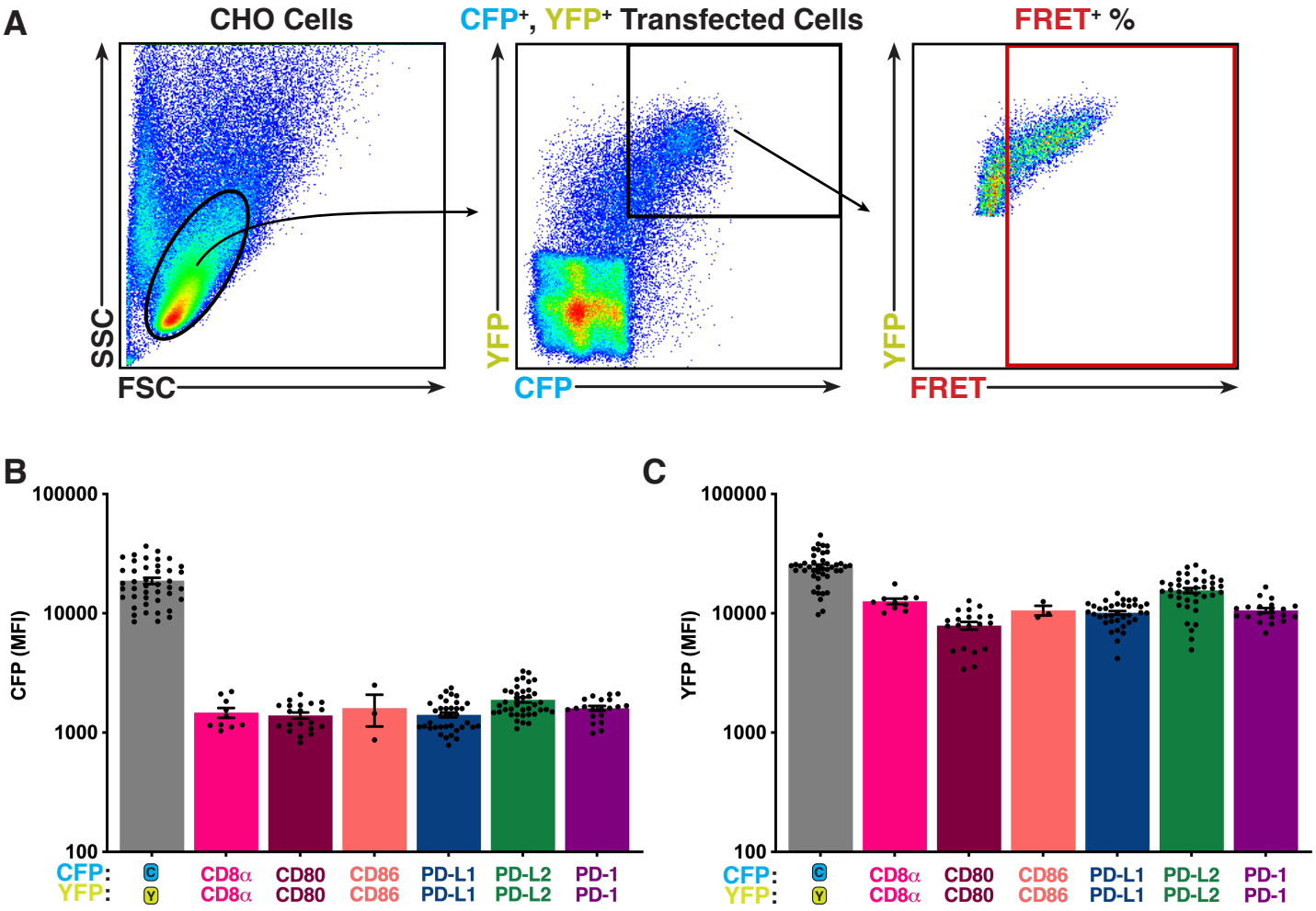

Supplemental Data Fig. 1. Flow-FRET gating strategy, expression controls, and PD-1 dimerization validation with FLIM-FRET and FCCS. (A) An initial gate selected healthy CHO cells based on forward and side scatter. A second gate was set to capture CFP^+, YFP^+ doubly transfected cells. Lastly, a gate was to set capture the population of doubly transfected cells that register as $FRET^+$ defined as YFP fluorescence above the indicated threshold (determined in Fig. 1A) when CFP was excited at 405 nm. (B and C) Expression levels measured via CFP and YFP MFI with excitation of 405 nm and 488 nm, respectively.

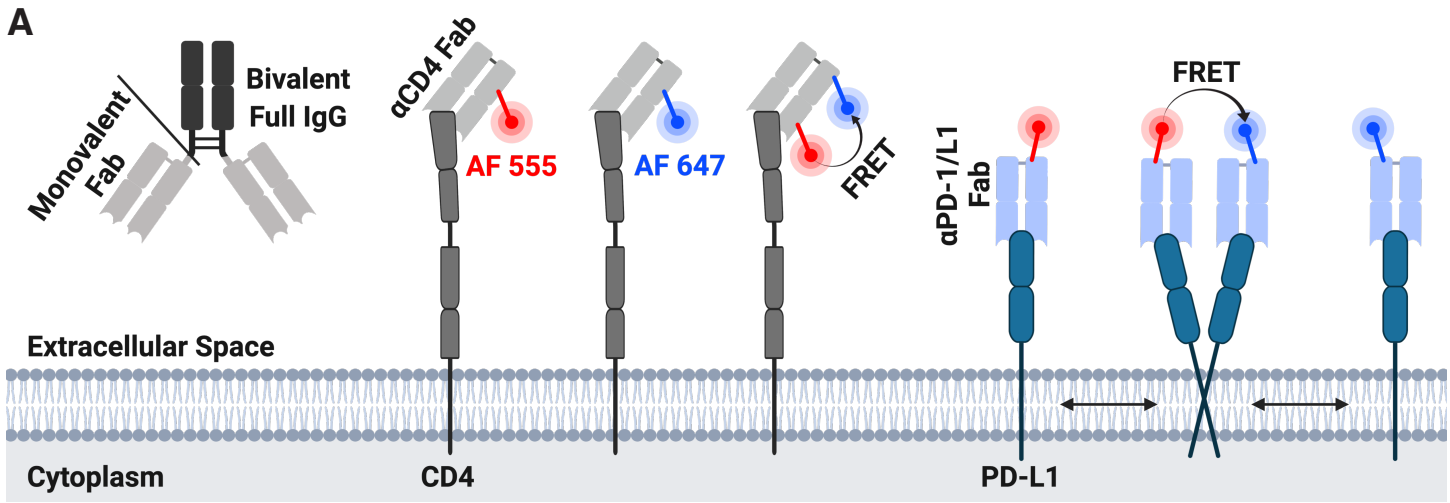

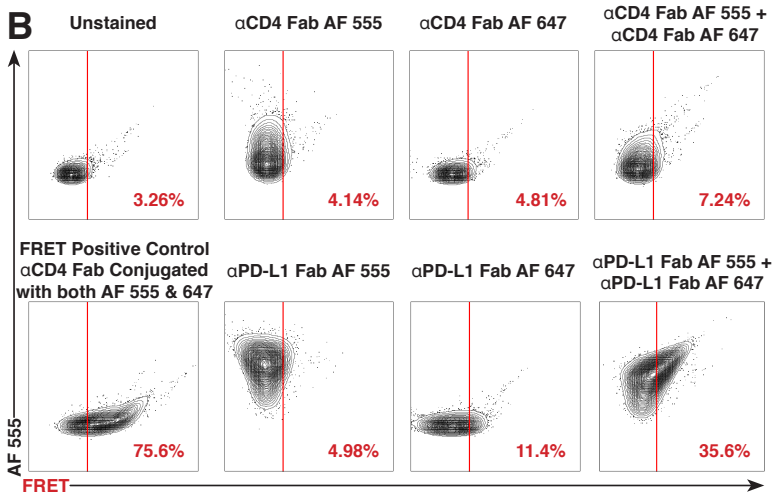

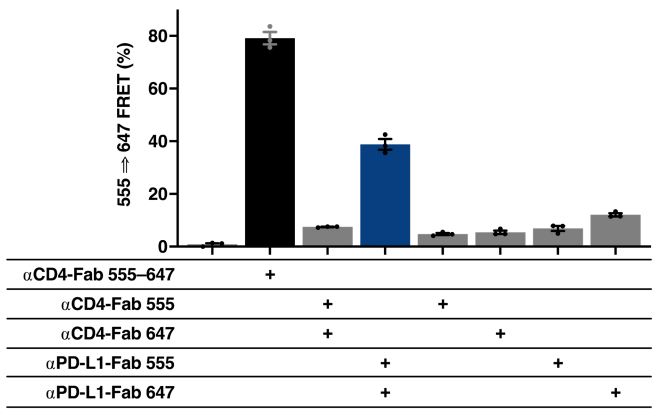

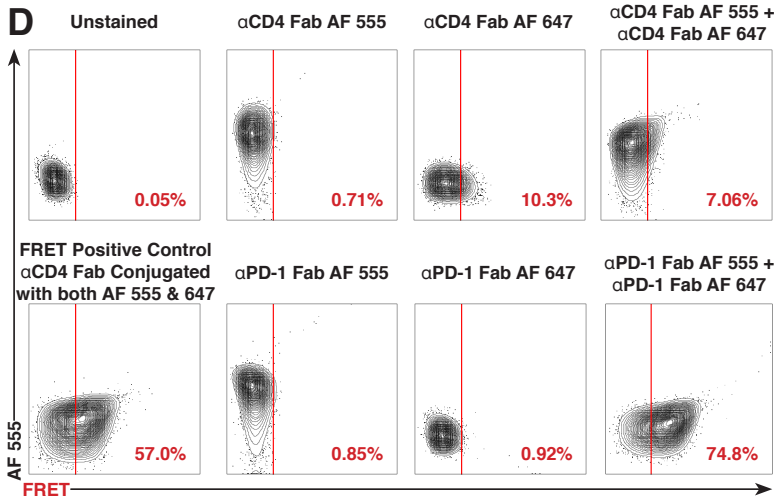

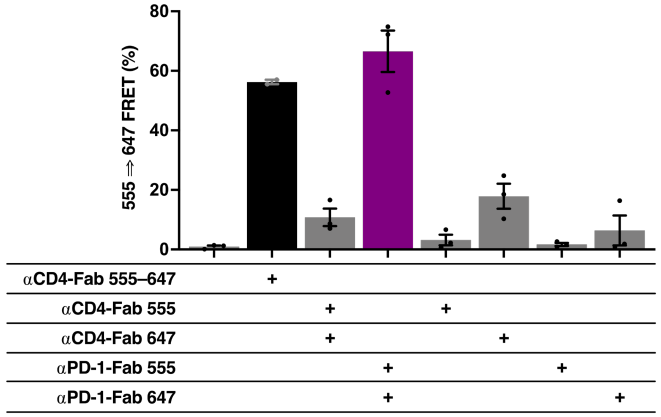

Supplemental Data Fig. 2. Endogenous PD-L1 and PD-1 homodimerization in *cis* on the cell surface. (A) Schematic of Fab staining to measure dimerization of endogenous immune receptors by flow-FRET. Fab fragments of mAbs directed to CD4 or PD-L1 were conjugated with AF 555, AF 647, or both and used to stain their cognate receptor. CD4 served as a control, monomeric immune receptor and dual staining with AF 555 and AF 647 served as a positive control for FRET (Created with BioRender). (B and C) HDLM-2 cells stained with anti-CD4 or anti-PD-L1 Fabs and analyzed for FRET by flow cytometry. (B) Cells are presented as a contour plot with the percent of cells scoring above the FRET threshold indicated. One representative experiment is displayed. (C) Summary of three independent experiments. (D and E) Activated Jurkat T cells stained with anti-CD4 or anti-PD-1 Fabs and analyzed for FRET by flow cytometry. (D) Cells are presented as a contour plot with the percent of cells scoring above the FRET threshold indicated. Data from one representative experiment are displayed. (E) Summary from three independent patient samples. Significance determined by paired t tests: * $p<0.05$, *** $p<0.001$, **** $p<0.0001$.

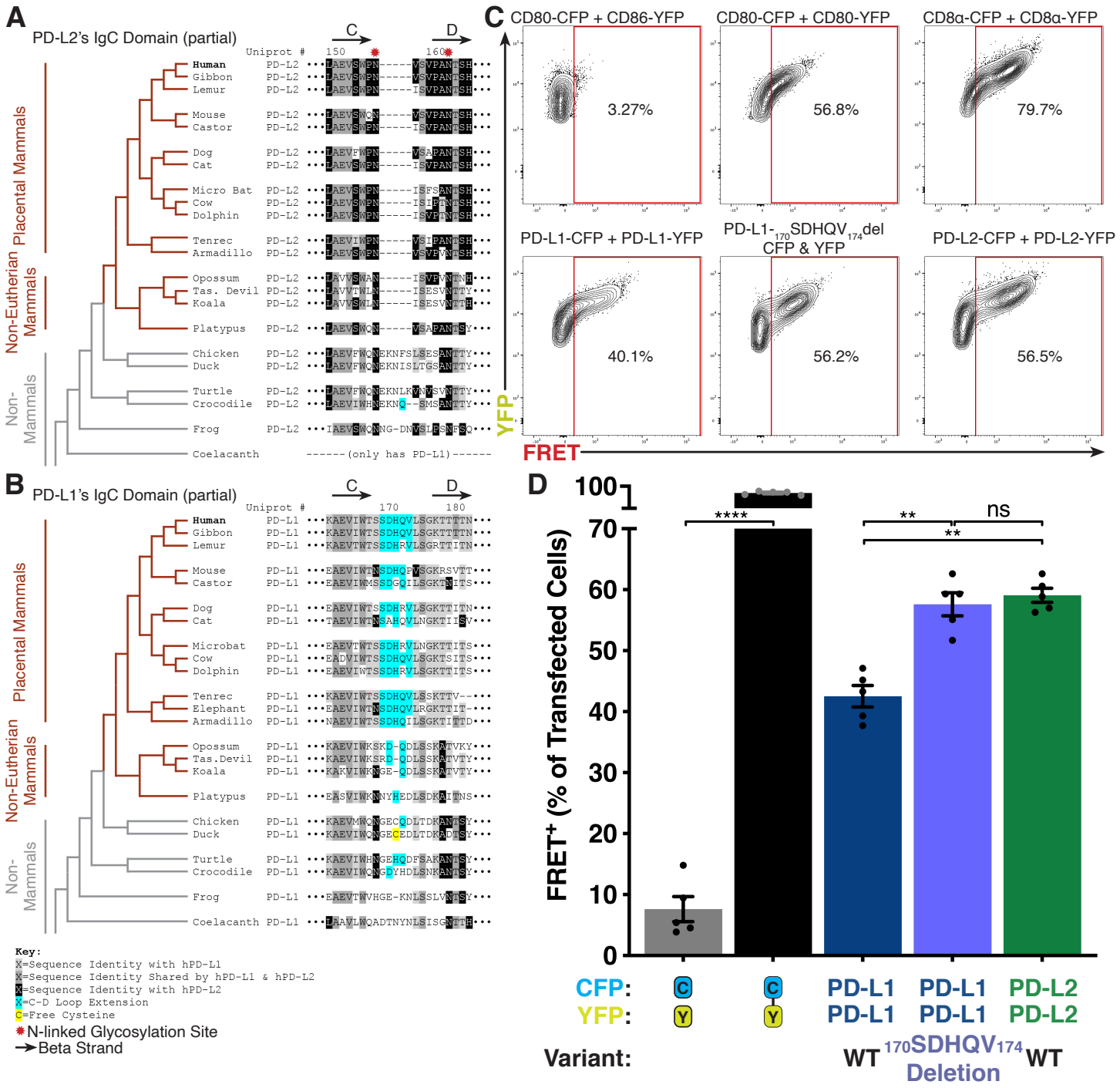

Supplemental Data Fig. 3. PD-L1 residues 170-174 in the membrane-proximal IgC domain weaken homodimerization. (A and B) Phylogenetic analysis of PD-ligand IgC domain C-D beta strand regions reveal that PD-L1 residues 170-174 (cyan) were lost in PD-L2 as mammals evolved. (C) Flow-FRET contour plots for CD80/CD86 (non-dimerizing), CD80 (dynamic homodimer), CD8α (stable homodimer), PD-L1, PD-L1-170-4$_{deletion}$, and PD-L2. The 170-174 deletion causes PD-L1 to convert from a dynamic to a stable dimer similar to PD-L2. (D) Cumulative flow-FRET data plotted as the percent of FRET+ transfected cells (n=5). Significance tested by paired t tests * $p<0.05$, ** $p<0.01$, **** $p<0.0001$.

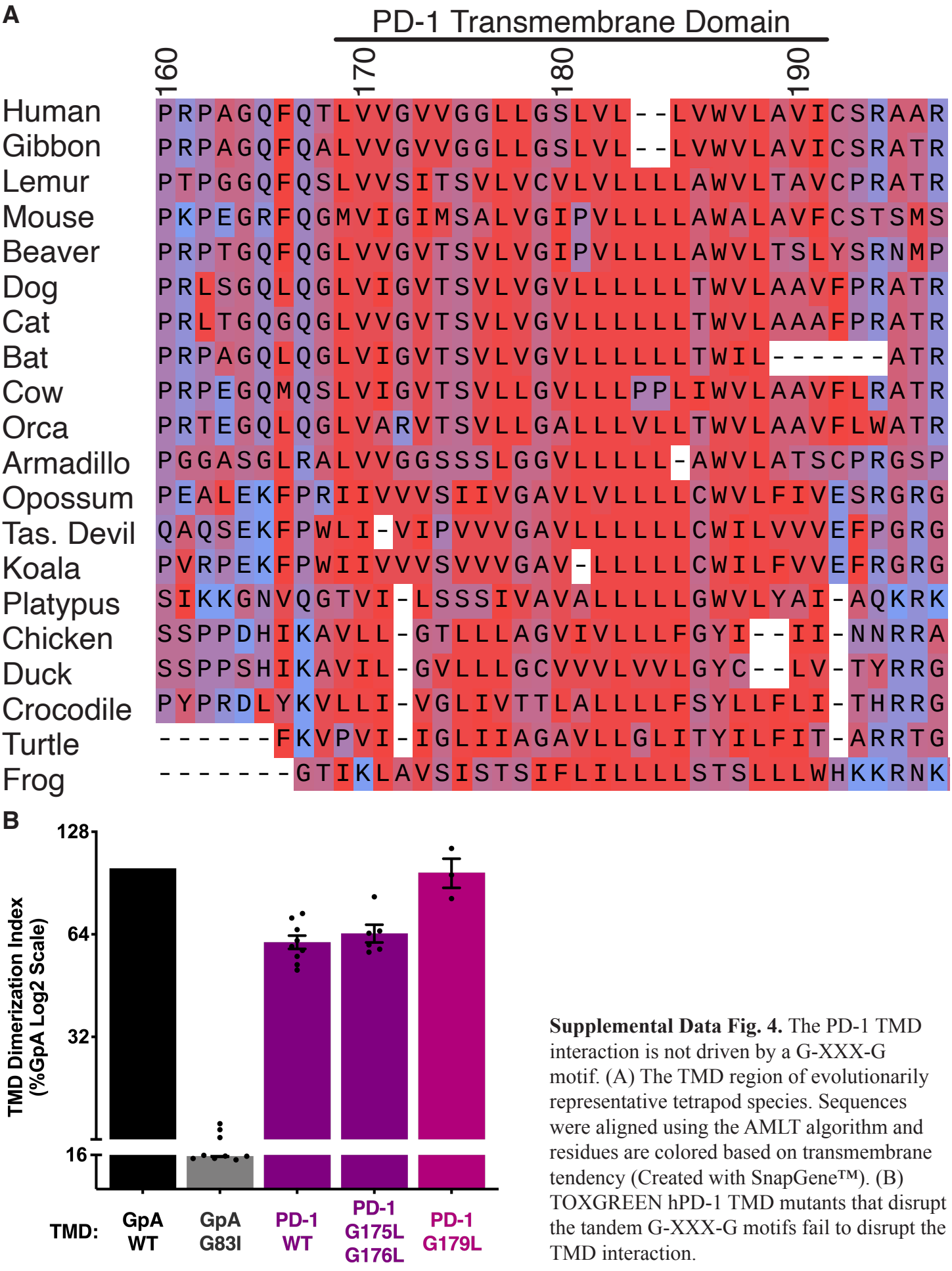

Supplemental Data Fig. 4. The PD-1 TMD interaction is not driven by a G-XXX-G motif. (A) The TMD region of evolutionarily representative tetrapod species. Sequences were aligned using the AMLT algorithm and residues are colored based on transmembrane tendency (Created with SnapGene™). (B) TOXGREEN hPD-1 TMD mutants that disrupt the tandem G-XXX-G motifs fail to disrupt the TMD interaction.

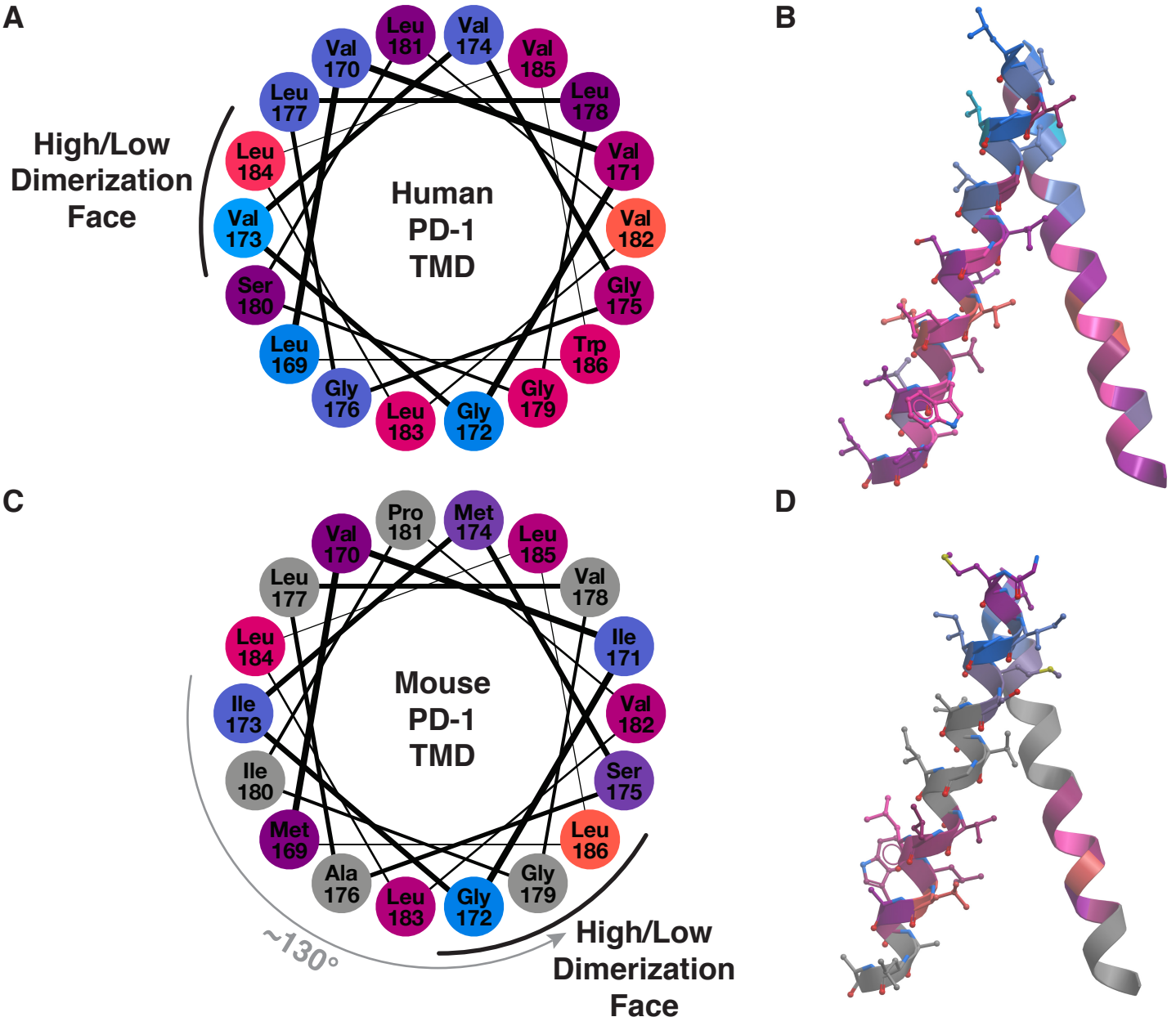

E

Similarity Coloring

Human: LVVGVVGGLLGSLVL--LVWVLAVI

Mouse: MVIGIMSALVGIPVLLLLAWALAVF

Trp Scan Coloring

LVVGVVGGLLGSLVL--LVWVLAVI

MVIGIMSALVGIPVLLLLAWALAVF

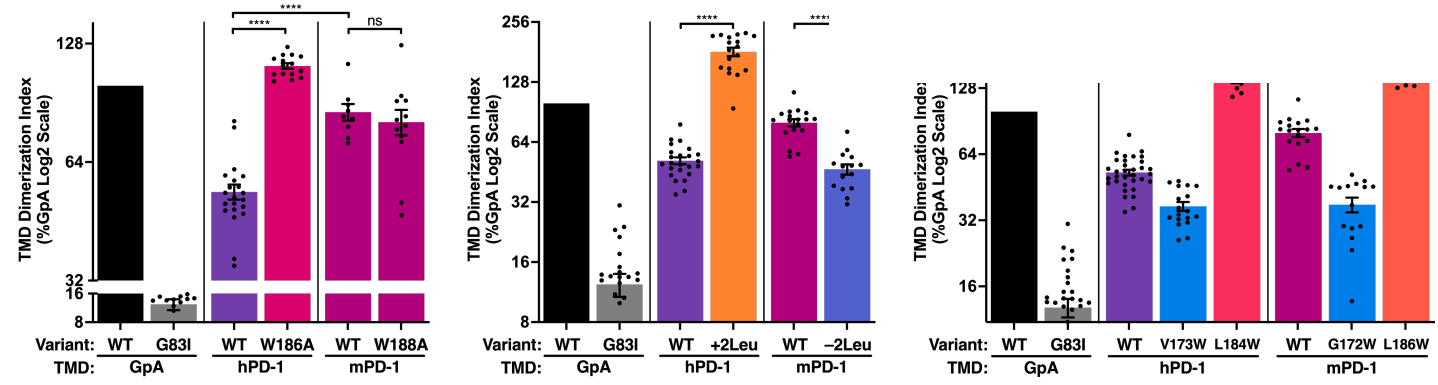

Supplemental Data Fig. 5. TMD interaction model of the human vs. mouse PD-1 TMDs and differential effects of substitutions for the native Trp and 2Leu TMD differences. (A-D) Human and mouse helical wheel (a and c, respectively) and "A" shaped helix dimerization interaction models (B and D, respectively) reveal a 130° shift in the dimerization face created by the 2Leu insertion in the murine PD-1 TMD. The "A" shaped models reveal the differential dispositions of the native Trp residues. The mouse model does not take into account the helical kink likely provided by Pro181. (E) hPD-1 versus mPD-1 TMD sequence comparisons by amino acid similarity (same residue indicated in black, similar residue indicated in grey, and different residue indicated in red) and Trp substitution effect (colors were assigned based on the log2 scaled color look up table in Fig. 4A and 4E). (F-H) Modulation of both human and mouse PD-1 dimerization with the indicated, analogous substitutions. Colors were assigned based on the log2 scaled color look up table in Fig. 4A and 4E. (F) Trp to Ala substitution (positions h186 and m188) enhanced human but not mouse PD-1 TMD dimerization. (G) Addition of two Leu residues in the human PD-1 TMD enhanced dimerization, whereas removal of two Leu from the murine PD-1 TMD diminished dimerization. (H) Analogous Trp substitutions into the human and mouse TMDs have similar effects generating low and high dimerization mutants used in functional experiments. Significance was determined by unpaired t tests: **** $p<0.0001$.

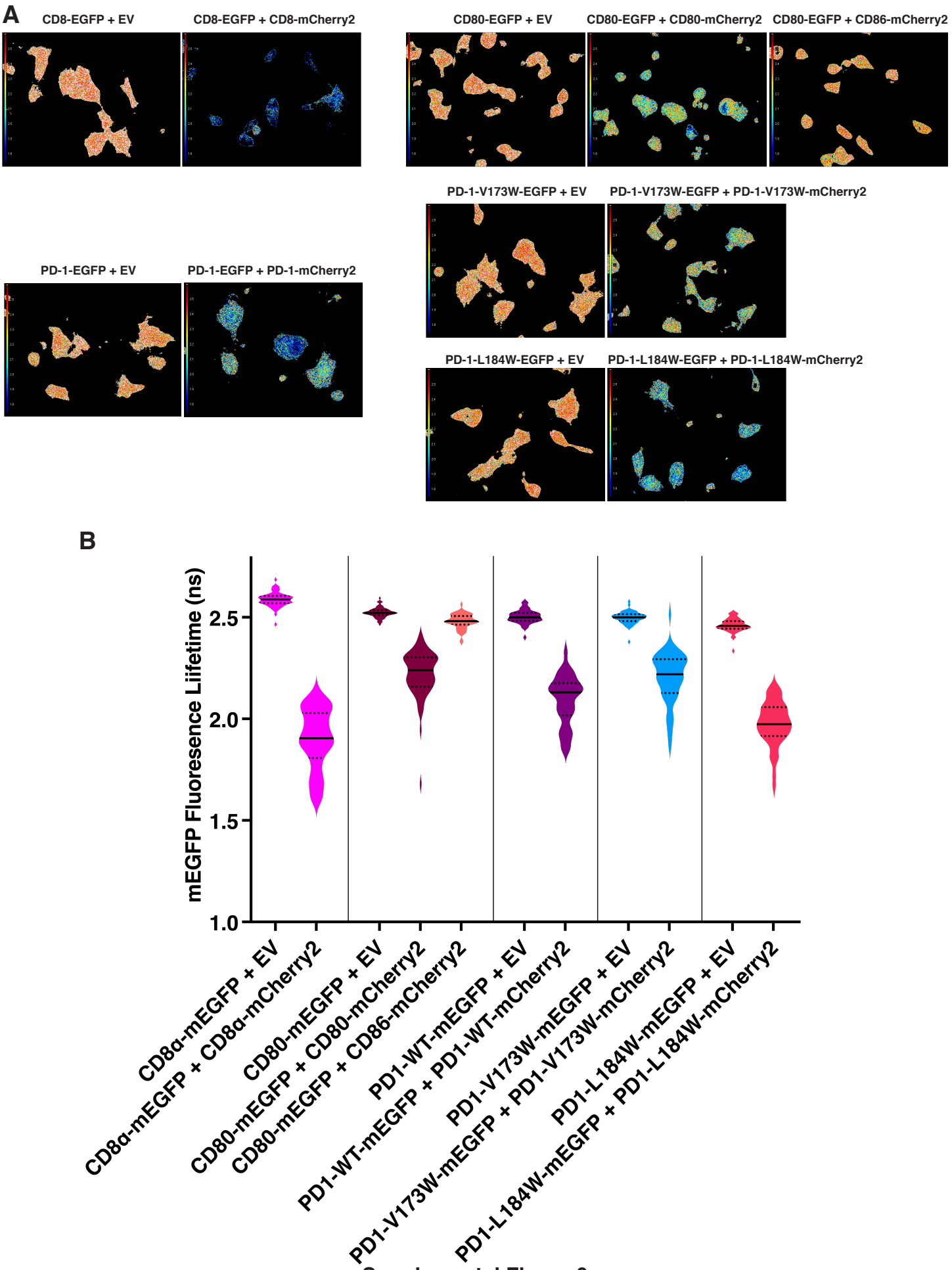

Supplemental Figure 6

Supplemental Data Fig. 6. Fluorescence lifetime imaging microscopy validates low and high PD-1 TMD dimerization Trp mutants. (A) Representative images of cells expressing the indicated proteins with pixels color-coded for mEGFP lifetime (red long, blue short). (B) Violin plot of mEGFP lifetime measurements of ≥60 cells transfected with the indicated plasmids (representative of three independent experiments).

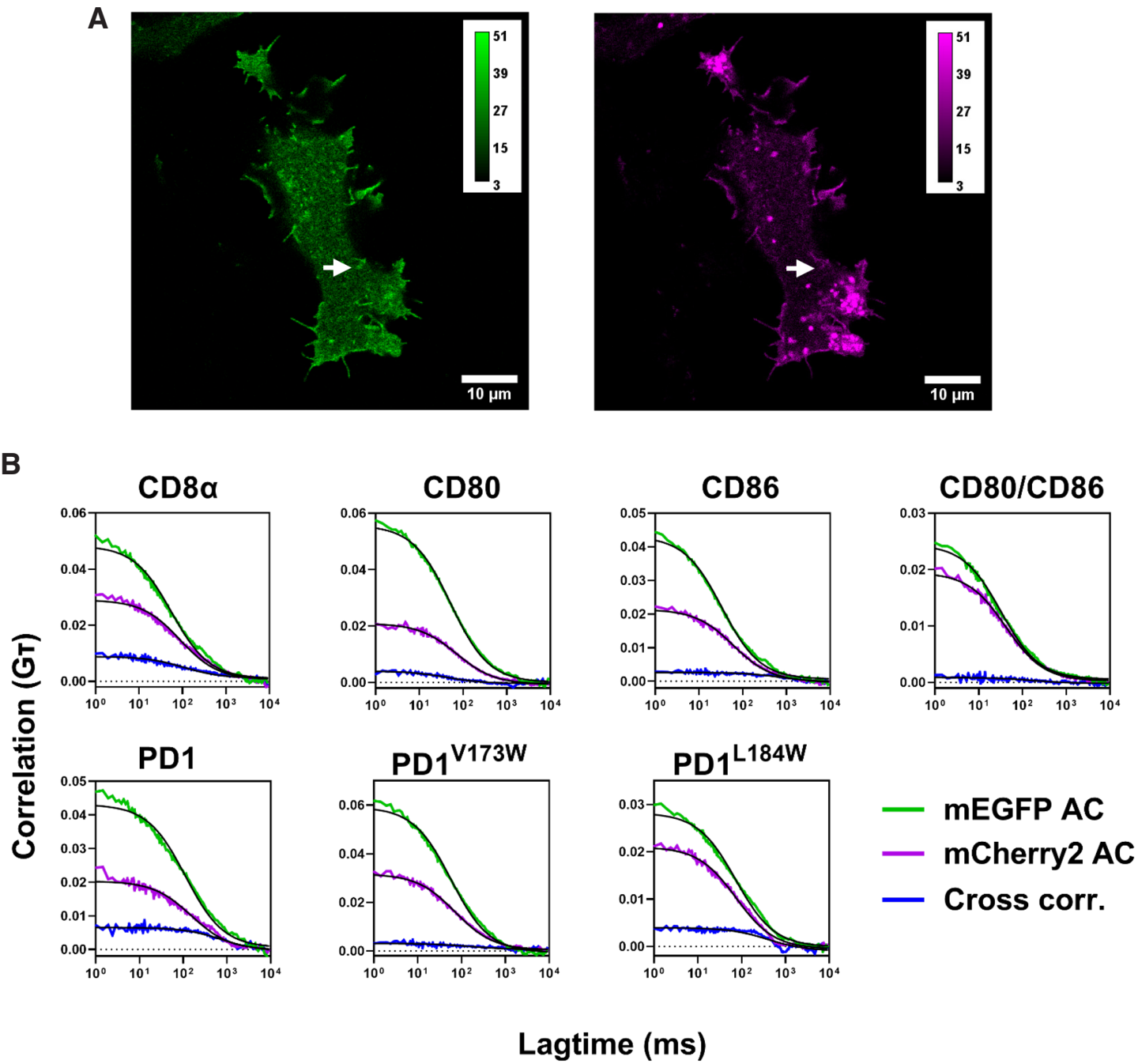

Supplemental Data Fig. 7. Fluorescence cross-correlation spectroscopy validates low and high PD-1 TMD dimerization mutants. (A) Representative confocal image of a HEK293T cell co-transfected with CD8α-mEGFP (left) and CD8α-mCherry2 (right) acquired in photon-counting mode with a pixel dwell-time of 12.62 µs. The calibration bar indicates the number of photons detected per pixel in each color. The arrows indicate the approximate position of the line-scan. The correlation curves from each of the 52 pixels in the line were averaged together for each cell measured. (B) Representative line-averaged FCCS curves are shown for one cell from each condition tested. Raw correlation curves are shown in color and fits are shown in black.

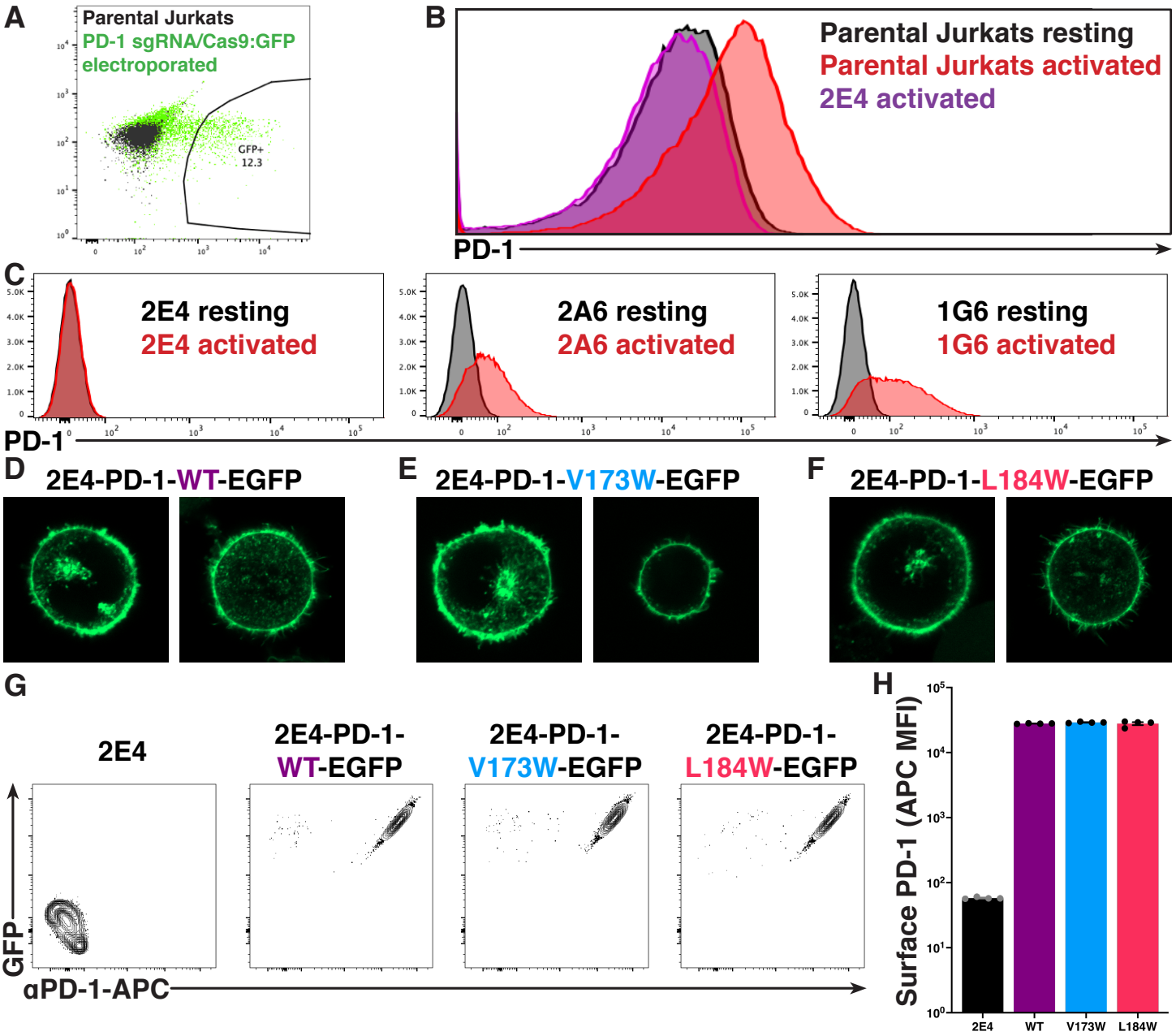
A
Parental Jurkats
PD-1 sgRNA/Cas9:GFP
electroporated
GFP+
12.3
B
Parental Jurkats resting
Parental Jurkats activated
2E4 activated
PD-1
C
2E4 resting
2E4 activated
2A6 resting
2A6 activated
1G6 resting
1G6 activated
PD-1
D
2E4-PD-1-WT-EGFP
E
2E4-PD-1-V173W-EGFP
F
2E4-PD-1-L184W-EGFP
G
2E4
2E4-PD-1-WT-EGFP
2E4-PD-1-V173W-EGFP
2E4-PD-1-L184W-EGFP
GFP
αPD-1-APC
H
Surface PD-1 (APC MFI)
2E4
WT
V173W
L184W
I
SHP2
PD-L1
Merge
pTyr
PD-L1
Merge
WT
V173W
L184W

Supplemental Data Fig. 8. Human PD-1 TMD dimerization impacts proximal inhibitory signaling within the immunological synapse. (A) Jurkat T cells were electroporated with PX458 directing expression of a PD-1 sgRNA, Cas9, and GFP and transformants cloned by single cell sorting for GFP expression. (B and C) Validation of PD-1 disruption in clone 2E4 but not 2A6 or 1G6 by staining for PD-1 before and after activation with anti-CD3 and anti-CD28 mAbs. (D-F) Confocal images of live 2E4 Jurkat cells expressing the indicated hPD-1-GFP fusion proteins (WT, low, or high dimerization, respectively). Two images are shown for each that correspond to Z sections at (*left*) or under (*right*) the Golgi. (G and H) PD-1 surface expression measured by flow cytometry of 2E4 cells and rescued variants stained with anti-PD-1-APC. (I) Representative TIRFM images of the supported lipid bilayer experiments shown in Fig. 5, A-C.

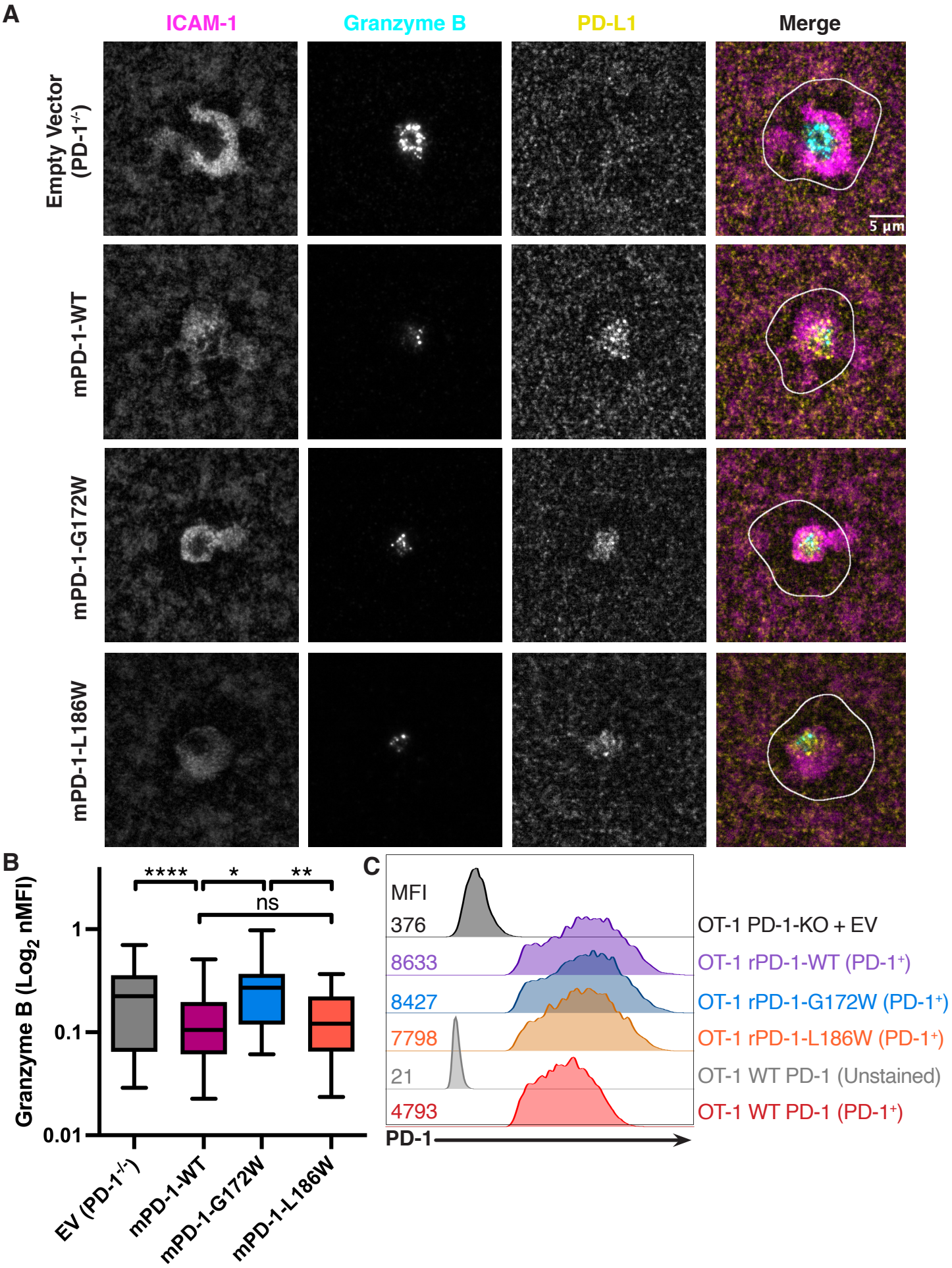
A
ICAM-1
Granzyme B
PD-L1
Merge
Empty Vector (PD-1-/-)
mPD-1-WT
mPD-1-G172W
mPD-1-L186W
5 µm
B
Granzyme B (Log2 nMFI)
****
*
**
ns
1
0.1
0.01
EV (PD-1-/-)
mPD-1-WT
mPD-1-G172W
mPD-1-L186W
C
MFI
376
8633
8427
7798
21
4793
PD-1
OT-1 PD-1-KO + EV
OT-1 rPD-1-WT (PD-1+)
OT-1 rPD-1-G172W (PD-1+)
OT-1 rPD-1-L186W (PD-1+)
OT-1 WT PD-1 (Unstained)
OT-1 WT PD-1 (PD-1+)

Supplemental Data Fig. 9. Immunological synapses formed by CD8 cells from OT1, PD-1$^{-/-}$ mice transduced with WT PD-1 or dimerization mutants. (A) CD8 T cells transduced with empty vector or the indicated PD-1 (as in Fig. 4) were applied to a supported lipid bilayer incorporating H-2Kb-pOVA, ICAM-1-AF405, and PD-L1-AF647, fixed and stained for granzyme B, and imaged by total internal reflection microscopy. (B) Normalized granzyme B release into the IS is depicted as box and whisker plots. Mean (solid line) and 10-90% range (whiskers) are indicated ($n \geq 86$). Significance was determined by Mann-Whitney test: * $p<0.05$, ** $p<0.01$, **** $p<0.0001$. (C) Comparison of PD-1 surface expression on retrovirally rescued (r) PD-1-KO OT1 cells and endogenous PD-1 expression of WT OT1 cells stimulated with anti-CD3/28 + soluble IL-2 for 24 hrs.

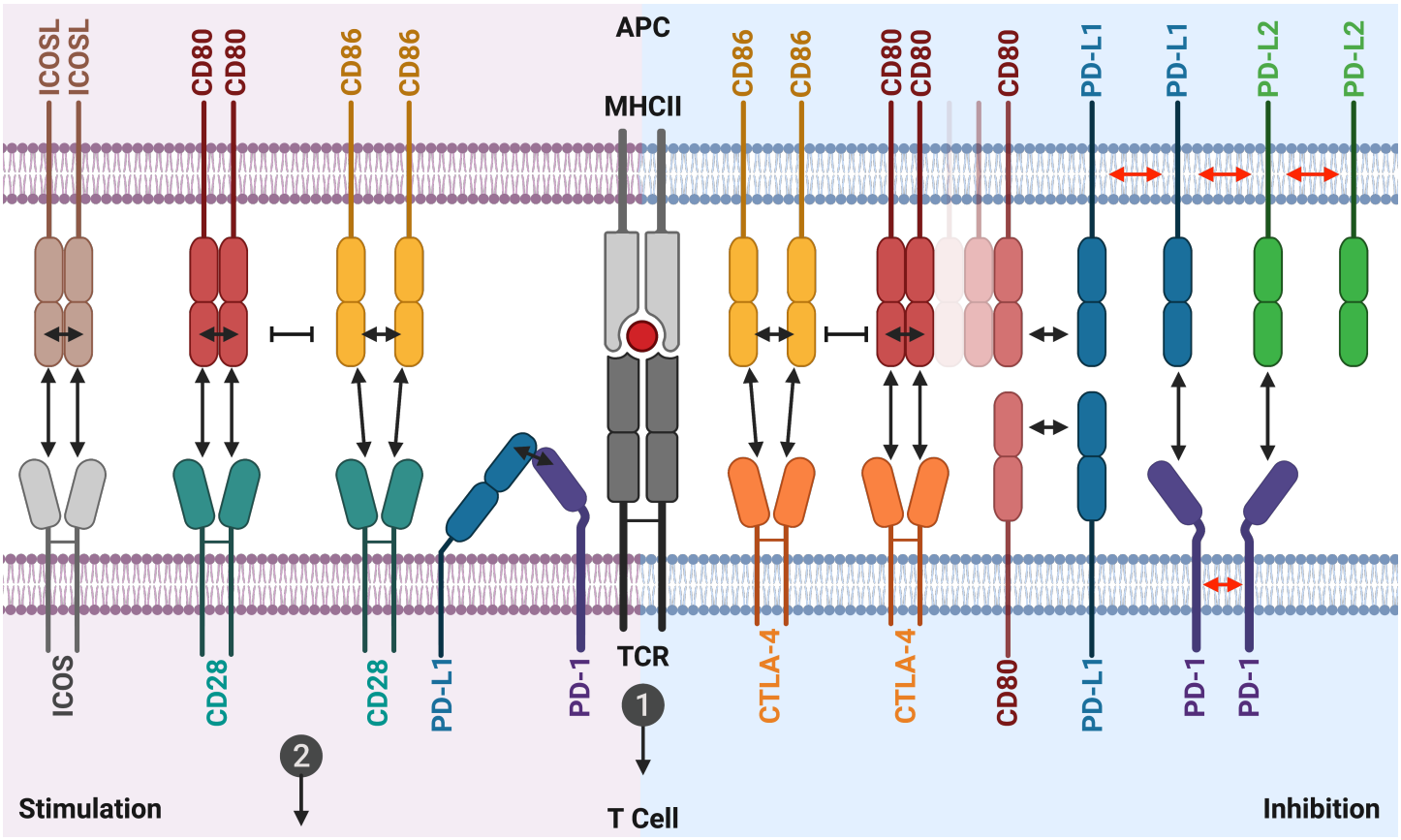

Supplemental Data Fig. 10. TCR signaling is controlled by co-stimulatory and co-inhibitory receptors that function via both *trans* and *cis* protein-protein interactions. Signal 1 from TCR signaling is insufficient to activate a naïve T cell. Co-stimulatory receptors provide signal 2. Co-inhibitory receptors counterbalance co-stimulation, limiting T cell activation. PD-1 is a member of the co-receptor family that includes CD28, CTLA-4, and ICOS. The PD-ligands are members of the B7-family that includes CD80, CD86, and ICOSL. These protein families interact via both trans and cis interactions that regulate T cell activation. Established interactions are indicated with black arrows. Previously unappreciated TMD *cis* interactions described in this study are indicated with red arrows. (Created with BioRender).